ADVANCED MATERIALS TECHNOLOGIES
www.advmattechnol.de

Addressable, Stretchable Heating Silicone Sheets

*R. Adam Bilodeau, Michelle C. Yuen, and Rebecca Kramer-Bottiglio**

Research into new active materials for soft robots has generated promising new thermally responsive materials for functions such as variable stiffness, on-demand shape change, and actuation. These new thermally responsive materials require a form of addressable thermal control that is compliance-matched to its host system. In response to this need, this work presents stretchable, addressable heating silicone sheets that can control soft, thermally responsive materials. The sheets are created using layer-by-layer deposition of a bulk conductive elastomer that can be Joule heated, with embedded liquid–metal microchannels used as electrodes. This combination allows the bulk, addressed material to be stretched and twisted while in operation. Local, addressable heating is demonstrated in a silicone-based composite that is capable of cyclic strains of up to 40%, while still self-heating to over 100 °C. The heating sheets are demonstrated as a thermal control platform in both color changing and stretch-and-hold operations using all silicone-based composites. Additionally, this platform is bonded to a variable-stiffness polymer that, with its selective heating capability, enables folding at targeted locations.

1. Introduction

Soft robotic systems are of great interest due to their robustness to impacts and vibrations, conformability to surfaces and objects, and potential to undergo large deformations due to low material stiffness. These advantages allow soft robots to fulfill functions such as grasping diverse and delicate objects, maneuvering around obstacles, or traveling over difficult terrain.[1–5] Research into new active materials for soft, highly deformable systems has yielded promising new branches of study, such as thermally responsive variable stiffness materials[6–8] and actuators.[9,10] Yet, these new thermally responsive materials require a form of thermal control that is compatible with the host materials. In this work, we present a stretchable, addressable silicone sheet that enables thermal control, and demonstrate its utility through integration with thermally responsive soft materials.

Many thermally responsive materials are utilized by the soft robotics community. Thermally softening polymers (such as thermoplastics and thermosets) are passively stiff, actively soft variable stiffness materials[6,11] that have been used in robotic systems for move-and-hold operations[12,13] as well as in conformable and on-demand structural systems.[7,14] Additionally, thermally responsive shape memory polymers and alloys have been employed as both stiffening agents and actuators.[6,8] Finally, thermally responsive silicone-based actuators have been recently developed, which undergo bulk expansion when trapped solvent is vaporized.[10] All of these previous examples required some thermal control, and so researchers have sought out ways to embed a close-contact heater where the compliance of the heater was properly matched with its thermally responsive material pair.[12,13,15,16]

In an effort to fill the need for compliance-matched thermal control, flexible and stretchable heaters are an active area of research, as are addressable heating structures and systems. Stretchable heating composite materials have been successfully developed with either conductive fillers or microstructures[17–21] and have demonstrated linear strains of up to 100%.[22,23] Proposed applications have included wearable technology and active therapy,[22,24–29] surface-based temperature control of nonplanar objects,[30] and thermo-chromatic flexible, and active microdisplays.[31–33] These examples, however, require high-complexity patterning techniques (e.g., lithographic masking) and often only heat up moderately. To facilitate thermal controllability across a 2D plane, researchers have begun to implement thermal addressability onto stretchable or flexible surfaces, in which only localized regions of the surface are heated.[34–38] These pioneering works have successfully implemented the concept, but they also require lithographic masking, complex assembly processes, high operational voltages (>100 V), or a fixed framework around only a few small pockets of thermally responsive material. Prior work has demonstrated stretchability and addressability in geometrically soft material systems (i.e., silicon-based electronics made stretchable through patterning crystalline materials onto prestretched silicone),[24,25] but to our knowledge, there has not yet been a combination of these two functions in a system which uses intrinsically soft materials (i.e., silicones and liquids). With our work, we combine the manufacturing simplicity gained from using a bulk silicone

R. A. Bilodeau
Purdue University
School of Mechanical Engineering
585 Purdue Mall, West Lafayette, IN 47907, USA
R. A. Bilodeau, Dr. M. C. Yuen, Prof. R. Kramer-Bottiglio
Yale University
School of Engineering and Applied Science
10 Hillhouse Avenue, New Haven, CT 06520, USA
E-mail: rebecca.kramer@yale.edu
The ORCID identification number(s) for the author(s) of this article can be found under https://doi.org/10.1002/admt.201900276.

DOI: 10.1002/admt.201900276

composite with the utility of a thermally addressed heating platform to gain the strengths from both sets of prior research.

Here we present a planar, stretchable, silicone-based Joule heating composite material strengthened by a pure-silicone support structure, with fluidic electrical interfaces, creating a robust "heater silicone" capable of stretching up to 40% while maintaining heater functionality. The support structure can be embedded with liquid metal wiring to enable an addressable electrical connection for localized Joule heating, which we use to demonstrate a mechanically robust, 2D thermal "pixel" display. This addressable heater sheet can be coupled with thermally responsive materials, such as variable stiffness and phase changing materials. In this work we show coupling of the heating composite to a variable-stiffness thermoplastic (polylactic acid, or PLA) or a thermally triggered, stiffness-changing silicone (wax–silicone composite), ensuring uniform heating of the adjacent material and enabling both reversible shape changes and stretch-and-hold operations. Finally, we demonstrate example systems comprising the addressable, stretchable heating sheet coupled to a uniform PLA sheet (with no pre-set mechanical hinges) reshaping in both two and three dimensions, showing how this platform opens up possibilities of on-demand origami folding in the future.

2. Manufacturing and Characterization of Heater Silicone Sheets

We first studied the effect of various manufacturing parameters of the bulk heater silicone material on its performance (i.e., electrical resistance as a function of applied strain). We then developed a compliant interfacing technique that enables heating while undergoing large deformations and demonstrate its utility and robustness by performing heating tasks while undergoing significant deformation.

2.1. Conductive Composite Electrical Characterization

The heater silicone is an electrically conductive composite made from expanded intercalated graphite (EIG) conductive filler dispersed in a silicone matrix, supported by a pure-silicone backbone, creating a monolithic, electrically conductive material sheet. EIG is an inexpensive filler formed by bulk exfoliation of graphene sheets from graphite flakes,[39,40] and has been used to create conductive composites in rigid-polymer composites,[41,42] including self-heating variable stiffness composites.[12] It has been used as a low loading (<15 wt% EIG) filler for stretchable, conductive elastomer composites and sensors,[43–45] and for our heater silicone we simply increased the loading (≥15 wt% EIG) to improve material conductivity. We adapted the rod-coating technique demonstrated by White et al.[45] to manufacture our composite (see **Figure 1**a), but coated multiple layers of conductive silicone on top of each other to increase the thickness of our conductive layer, reducing the overall sheet resistance in our samples. To create the heater silicone in a stretchable, sheet form, we encased the initial conductive composite in a pure silicone backbone (a strengthening support that bonds through the composite), increasing the cyclic stretchability of the composite

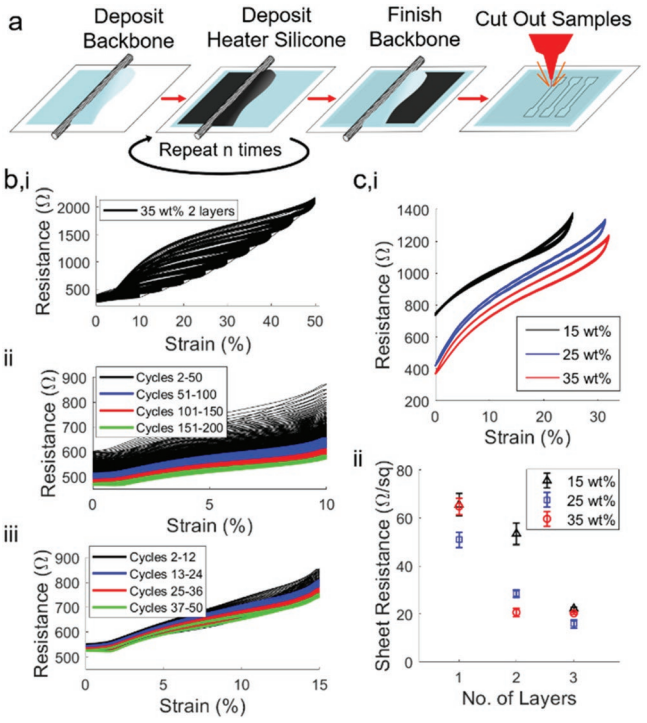

Figure 1. Manufacturing steps and electrical characterization data from the strain tests performed on high aspect ratio samples of the heater silicone. a) Multiple layers of EIG composite silicone are deposited onto a neat silicone backbone to create the heater silicone sheet, and samples are cut out of the sheet with a laser cutter for electrical testing. b,i) An example of a cyclic test dataset (sample design parameters: 10 cm × 1 cm, 35 wt% EIG, n = 2 layers). b,ii–b,iii) cyclic tests focusing on 10% and 15% strain (10 cm × 1 cm, 15 wt% EIG, n = 2 layers) with the same y-scale and color distinguishing test cycles (1st cycle always omitted). c,i) Representative resistance-strain curves from heater silicone samples (10 cm × 1 cm, n = 3 layers) with different concentrations of EIG. Curves show the final 10 repetitions of a 50-cycle test (steady-state response). c,ii) Sheet resistance of unstrained heater silicone with different concentrations of filler and increasing numbers of layers.

(embrittled from the high filler loading) with minimal impact on conductivity (see Figure S1, Supporting Information).

We performed a detailed characterization of the electrical resistance of the heater silicone under cyclic strain, while varying several manufacturing and design parameters. In Figure 1, we highlight some of the results from varying two key manufacturing parameters: the weight percent of the expanded intercalated graphite (EIG) filler (15, 25, and 35 wt%), and the number of layers of the heater silicone (n = 1, 2, or 3, based on the number of times we rod coated the heater silicone onto the sheet). The thickness of the conductive layer varied between 52 and 300 µm and was dependent on both the filler ratio and the number of layers (Figure S1, Supporting Information). We also varied the design of the heater silicone sheets by including a silicone backbone reinforcement on one-side or both sides of the conductive composite, and those results and comparisons can be found in Figure S1 in the Supporting Information. We tested three samples at each level of each design parameter, for a total of 54 samples tested. Figure 1b,i is an example of a dataset collected for a single sample with the following parameters: 35 wt% EIG heater silicone concentration, two layers of

heater silicone coated onto the sample, and a backbone on both sides of the material.

Each sample was mounted in a materials tester (Instron 3345) and clamped using an electrically conductive clamp to measure the resistance of the sample in situ. Samples were cyclically strained 200 times to 10% strain and then strained 50 times to incrementally higher strain values (5% strain increase per increment, making the test 15%, 20%, 25%, etc.). The reason for the decrease in cycle count at higher strains is based on the material more rapidly reaching a steady-state strain response after the 200 cycle "break-in." Initially, at 10% strain, the samples would undergo a lengthy settling response (see Figure 1b,ii) and so we cycled the sample to ensure that the sample's resistance had settled before testing at higher strains. After that initial break-in, each sample settled after about 40 cycles (see Figure 1b,iii), and so all comparisons of sample performance were based on the resistances measured in the last set of 10 cycles (cycles 41–50) at each strain value. We note that the overall decrease in resistance during cycling is an interesting characteristic of the composite material. We suspect that the decrease is due to a combination of the porosity of the material, slow alignment of the disk-like EIG particles during a (relatively) slow strain of the material, and viscoelastic effects of the silicone undergoing constant strain cycling.

The last 10 cycles of three samples are plotted in Figure 1c,i. Each sample shown was manufactured with the same number of conductive layers but, by increasing the loading, the initial (unstrained) resistance of the samples decreased, as did the resistivity of the sample over the entire strain curve. We also observed that the backbone allowed us to repeatedly strain samples over 25% while maintaining a good electrical resistance for Joule heating (for additional information, see Figure S1, Supporting Information). Although the lowest weight percent (15 wt% EIG) showed a significantly higher resistance (at lower strains), this did not make it ineligible for use as a Joule-heating material. Instead, we altered subsequent sample geometries to take into account the higher initial resistance. Figure 1c,ii shows that, all other parameters held constant, increasing the number of layers resulted in a decrease in the overall "sheet resistance" of the material. This holds logically, since sheet resistance does not consider the thickness of the conductive layer, whereas overall resistance is a volumetric property, and, therefore, effected by material thickness. The material characterization performed here enabled us to select which manufacturing and design parameters to use, based on the desired geometry or stretchability goals, while performing the subsequent experiments.

2.2. Liquid Metal Interfacing and Localized Heating

To create stretchable electrodes that can connect to the heater silicone, we embedded soft wiring directly into the supporting backbone using a eutectic gallium–indium–tin alloy (galinstan) as conductive (conductivity = 3.4×10^4 S cm^{-1})[46] stretchable wiring. Galinstan is liquid at room temperature allowing it to bend and stretch with the surrounding silicone.[46,47] Additionally, the liquid alloy is stable at the elevated temperatures used in our heater, preventing electrode burnout problems.

While experimenting with stretchable liquid metal wiring, we qualitatively noticed that liquid metals interfaced better with the heater silicone as compared to copper wire, i.e., the system had a reduced overall resistance. To confirm our observations, we performed a simple test to measure the difference in resistance for a sample of material with a copper wire electrode and a liquid metal electrode of the same geometry, as demonstrated in Figure S2 in the Supporting Information. The liquid metal electrode dropped the contact resistance by over 10 Ω, when compared to the uncompressed wire connection (see Figure S2 in the Supporting Information for more details). The numeric value of this improvement depends heavily on the geometry of the heater silicone sample and the electrode connection, but in the subsequent examples we present throughout this work, the reduction of contact resistance greatly improved our ability to evenly heat the planar silicone sheets.

To improve the functionality of the heating silicone, we wanted to be able to do more than just heat the whole system from end-to-end, but also at select locations in the body. We used direct filament casting to embed conductive wiring throughout the heater silicone so that we could create soft, localized contacts and, therefore, heat targeted areas of the conductive silicone sheet. Li et al. demonstrated a direct filament casting method to create high-resolution liquid-metal circuits in parallel, in an additive-based manufacturing processes.[48] By placing a filament during the silicone casting process where a liquid-metal channel is desired, hollow channels are created in the cured silicone once the filaments are removed which can then be filled with liquid metal. We implemented this method using copper wire as our filament (28–30 AWG, 0.25–0.3 mm dia) and embedded the liquid metal channels directly into the heater silicone backbone.

In **Figure 2** we show the results of casting two types of liquid-metal channels during the heater manufacture. Since we used a wire as the mold for the electrode traces, the electrodes could be shaped into nearly any 2D shape we desired (so long as the wire can be removed after casting). For this work, we used U-shaped and straight-line electrodes to apply an electric field in the heater silicone between two parallel lines and two points, respectively, which allows us to change the type of heat addressability between heating a swath of silicone, to focusing the heat on a single spot (see Figure 2). The spot-heat sample in Figure 2 was designed with the liquid metal line embedded into the conductive composite; therefore, the tear-drop shape is due to Joule heating along the entire liquid metal line. This inspired us to move the liquid metal lines to be fully embedded in the backbone (except at the spot-heat location) to reduce the electrical contact between electrode and heater.

2.3. Stretchable Heating

To corroborate the results of the electrical characterization, we performed cyclic strain tests on samples of the heater silicone while Joule heating them to over 100 °C. We chose to test shorter samples than in our electrical tests (with a

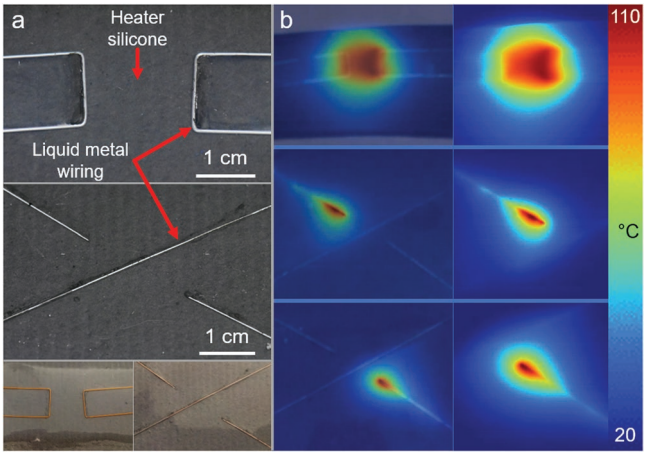

Figure 2. Two different liquid metal channels cast into the heating silicone, and their corresponding effect on the way the material heats up. a) Top: Two parallel line electrodes create a heat "patch" over an area. Middle: Liquid metal channels ending at point create a point of heat. Bottom: photographs showing the copper wires cast into the silicone to create the channels. b) The left column has a semi-transparent IR image overlaid on a visible light image of the heater silicone/liquid metal line pattern. The right column is a zoomed in view of the IR image.

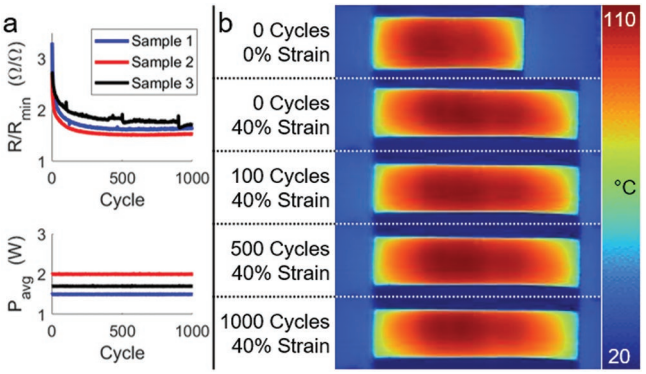

Figure 3. Results from cyclic strain tests while Joule heating samples of heater silicone. a) The normalized, average resistance of the sample in each cycle, as well as the average power required to Joule heat the sample, presented against the cycle number. The plateau in the resistance curve and the flat power consumption indicate good sample health throughout the tests. b) IR images of one of the samples tested, at 0% strain and then at the maximum strain (40% strain) over the 1000 cycle period, showing little-to-no degradation in the sample's ability to evenly heat. Sample heating area is ≈3 cm × 1 cm at 0% strain.

3:1 aspect ratio), and so we were able to use the 15 wt% EIG loading to improve the uniformity of the heating at high strains. We designed a custom straining device that allowed us to use liquid metal contacts to Joule heat only the portion of the heater silicone experiencing a uniform strain field. This removed any effects of clamping on the sample's electrical performance, so we could focus on the effects of linear strain on the sample's ability to Joule heat. Preliminary pull-to-failure tests revealed that the heater silicone could robustly support 40% strains while continuing to uniformly heat up to over 100 °C. We then performed cyclic tests on fresh samples, cycling them to 40% strain, while continuously Joule heating them to over 100 °C. Figure S3 in the Supporting Information has more details on our strain setup, as well as the preliminary pull-to-failure tests.

Figure 3 shows the results of the cyclic tests for three samples, as well as IR images of one of the samples tested. Both the normalized, average resistance and the average power consumed by the samples are shown over the 1000 cycles. The sample resistance was calculated from the voltage and current draw (as measured by the programmable power supply) and, unsurprisingly, increased while the samples were strained and decreased while the strain was being released. The average resistance of each cycle is presented in Figure 3a, normalized by the lowest resistance value of the final cycle. As expected from the electrical tests (see Figure 1), the samples each show a steady decrease in their resistances until they plateau after 100–200 cycles for the remainder of the 1000 cycles. Uniform power consumption of the samples (Figure 3a), paired with the sample maintaining the same temperature, (Figure 3b) acts as a good initial indicator of the health of each sample throughout all 1000 cycles (see Figure S3 in the Supporting Information for more details). Occasional spikes and drops in the calculated power (due to the power supply) were smoothed out by taking the average power consumed within each cycle. Figure 3b shows the IR image from one of the samples that, after 1000 cycles, shows no difference in its heating pattern when compared to its initial first cycle. Additionally, a quantitative analysis of the centerline temperature of the sample is plotted in Figure S6 in the Supporting Information for the IR images in Figure 3b, showing the sample's consistent temperature profile throughout the entire cycling process. From this test, we concluded that, when properly manufactured, the heater silicone functions well over 1000 cycles. Additional details are discussed further in Figure S3 in the Supporting Information.

3. Implementation in Silicone-Based Material Devices

The utility of our heater silicone arises from its stretchability and addressability, allowing it to be seamlessly embedded into "all-soft" systems. We demonstrate these attributes by integrating thermally responsive silicones with the heater silicone platform to create both stretch-and-hold operations and color changing functionality.

3.1. Stretch-and-Hold Operations

To demonstrate the utility of a repeatably stretchable, silicone-based heater, we performed some basic stretch-and-hold experiments using a silicone-based, variable elasticity "wax silicone" (see **Figure 4**). The wax silicone is a composite of paraffin wax microparticles embedded into a silicone matrix. At room temperature, the wax is solid and increases the silicone's elastic modulus. When the wax melts, the silicone is "softened" and can stretch like any other closed-cell silicone foam. If the wax is cooled (and solidified) while the silicone matrix is stretched, the solidified wax inclusions hold an elongated shape, preventing the silicone matrix from relaxing back to its original

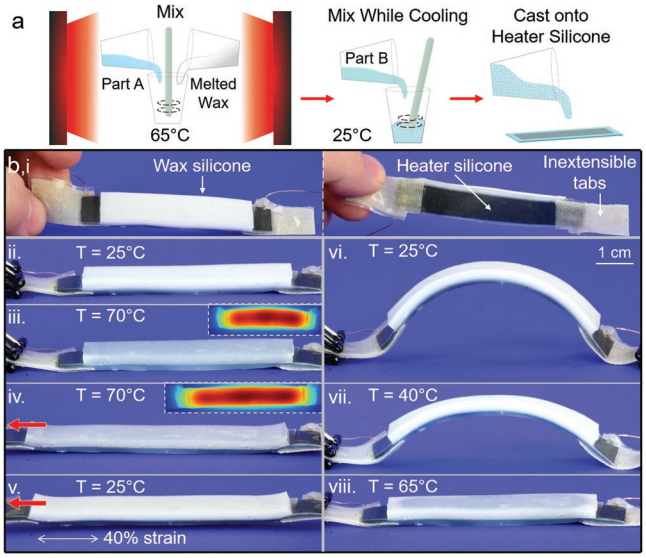

Figure 4. "Stretch and hold" shape change. a) Manufacture of the temperature-sensitive wax–silicone composite that leverages the low temperature phase change of wax to hold a new length when cooled while stretched. b,i) a sample of heater silicone bonded to wax silicone used for this demonstration, with inextensible tabs to allow for an even straining of the heater silicone while reinforcing the liquid metal electrical contacts. b,ii–viii) the sequential steps as the system starts from cooled state, is heated to melt the wax silicone, stretched, cooled to solidify the wax silicone, allowed to relax (with the wax silicone holding its extension), and then reheated to re-melt the wax silicone and restore it to its unstrained state.

length. After this, when the wax is re-melted, the silicone's restoring elastic force allows the system to return to its original, unstrained length.

We cast the wax silicone onto our heater silicone to create a material system capable of stretch-and-hold operations. In Figure 4a, we demonstrate the basic process used to make this stretch-and-hold composite. We mixed melted wax by hand into a heated Part A of the two-part silicone pre-cure at a high enough temperature to keep the wax melted. The mixture was then cooled by mixing in a room-temperature Part B, creating solid wax particulates, and cast onto the heater silicone. Once again, the backbone of our heater silicone provides an additional advantage as it bonds very well to the wax silicone's matrix. Figure 4b shows both the final sample used (with inextensible tabs to pull from and liquid metal electrodes (not visible)) as well as a fully reversible stretch-and-hold cycle, described as follows. The heater silicone melts the wax (resulting in a translucent color change in the wax silicone), and the composite system is stretched while cooling the wax silicone. Once cooled and released, the system pops up out-of-plane to obtain a minimum energy state between the heater silicone's restoring elastic compressive energy and the wax silicone's elongation. To restore the original state of the system, we simply reheat the heater silicone to melt the wax. At this point, the stretch-and-hold cycle can begin anew. We repeated this cycle several times, achieving a pop-up structure each time with no observable degradation in the heater silicone between cycles. One cycle is demonstrated in Video S1 in the Supporting Information.

3.2. Robust, Addressed Spot Heating

Having successfully demonstrated both the stretchability and the addressability of our heater silicone sheets, we then created a 2D addressed heater with rectangular arrays of spot heating "pixels" (shown in **Figure 5**a). Each pixel in the array was capable of heating locally to above 100 °C, and the system could be stretched and manipulated during operation. To get this 2D array of localized contact points, the liquid metal wires had to overlap the active area of the heater silicone. As mentioned previously, the bottom-up heater silicone sheet manufacturing allowed us to lift the liquid metal wiring out-of-plane from the conductive composite silicone (see Figure 5b). After the conductive composite cured, copper wires were gently placed on top and droplets of the composite were deposited at each pixel, connecting the copper wire at these locations to the bulk heater underneath. As the silicone backbone was cast on top to finish the heater silicone sheet, liquid silicone seeped under the wires, separating the rest of the electrode's channel from the conductive silicone with a thin, nonconductive barrier. Once the wires were removed and the channels filled with liquid metal, the only connection between the liquid metal traces and the planar heater was at the individual points. To control the activation of each pixel, we designed a high current PCB which could switch each channel between a high-voltage state, ground state, or a neutral ("floating") state (see Section S4, Supporting Information).

To demonstrate one application of this heating array, we created a mechanically robust digital thermal display. To elicit a response in the visible-light spectrum from the display, a layer of silicone loaded with thermochromic pigment was added on top of the heater patterned with a 4×5 pixel array in a 2 in $\times$ 1.5 in rectangle (5.1 cm $\times$ 3.8 cm) (see Figure 5c). We activated groups of pixels and showed that we could both heat the whole area or cause various letters of the alphabet to appear (see Figure 5d and Video S2, Supporting Information). Since the whole system was made of silicone composites, we were able to change the orientation and folding direction of the display while it was changing letters. Additionally, to test an increased density of heating pixels, we manufactured a higher density pixel array with 6×6 pixels in the same active rectangular region as the 4×5 pixel display. This increased the pixel density from 1 to 1.9 pixels cm^{-2}. We used this higher-density array to demonstrate the robustness of the system to external perturbations, by both crumpling and stretching the display, while it continued to display different letters (see Figure 5c,vi and Video S3, Supporting Information). Though a thermally responsive, color changing display may seem limited in utility, we see additional applications for digitally controllable, stretchable, color changing silicones in situations similar to those presented by Morin et al., who added visible light camouflage to their soft actuators by actively changing the color of the silicone by injecting colored fluids into their actuator.[49]

4. On-Demand Shape Change

After demonstrating the robustness of the heater silicone and its addressable heating functionality while undergoing

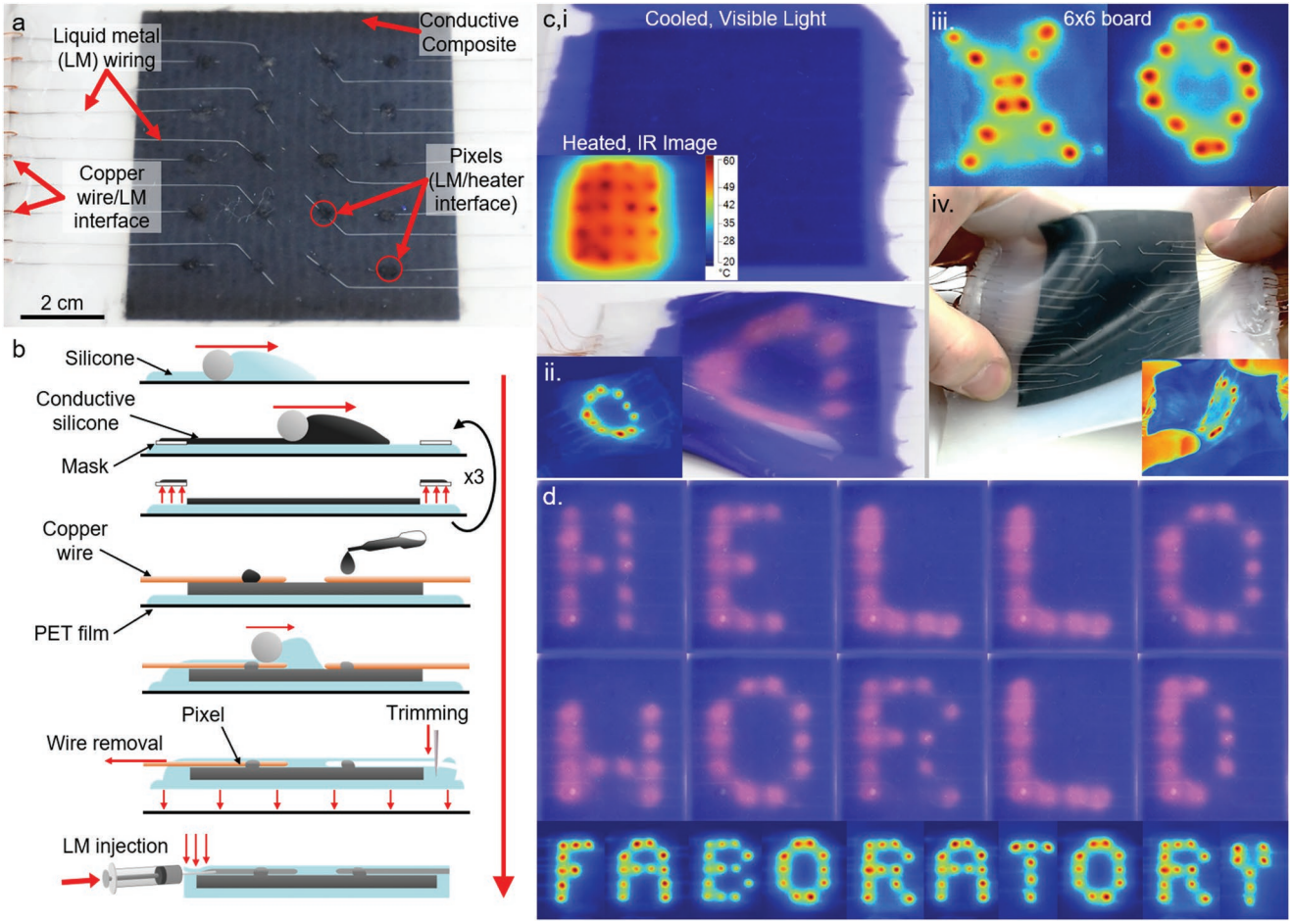

Figure 5. a) A visible light image of our fully soft 2D addressable heater composed of a heater silicone square with liquid metal electrodes. b) Manufacturing the 2D addressable heater pixel interfaces by adding a droplet of heater silicone at the location of interest on the wire molds. The liquid silicone seeps under the wire separating the rest of the liquid metal channel from the conductive composite. c,i) The 2D addressable heater with a temperature-responsive silicone laid on top (visible and IR images). c,ii) The addressable heater functions even when warped/flexed during operation (visible and IR images). c,iii) a higher-density board with 36 pixels (6 × 6) in the same form-factor as the 4 × 5 board, showing several letters. c,iv) The 6 × 6 board remains active while experiencing a large deformation stress. d) Visible light images of the automated system printing out the letters "HELLOWORLD" consecutively, and IR images of other letters captured, and organized to spell "Faboratory".

deformations, we desired to implement the platform in reversible shape changing structures. To do this, we used the heater silicone to soften a variable stiffness material (PLA) and demonstrated several shape-change modes in the variable stiffness sheet. Additionally, we integrated the addressable heating to selectively soften regions for on-demand shaping and folding.

4.1. Reversible Shape Change

To create reversible shape change (and shape holding), we bonded the heater silicone to the PLA using a robust epoxy bond, resulting in a composite heater/variable stiffness material (see **Figure 6**a, and Figure S5 and S6 in the Supporting Information for more details).[7,13] Since the bonded heater silicone can both stretch and compress without loss of bond integrity or functionality, the system could maintain elevated temperatures for reshaping and then be cooled to hold the new shape (see Figure 6b,i). It also allowed us to reheat the shaped PLA to reverse the shape change. Though the heater silicone could heat the PLA sheet to 150 °C, when the PLA's temperature increased above 65 °C we could begin to reshape the sheet (see also Figure S7, Supporting Information). Various shapes were imparted onto the sheet including smooth curves (Figure 6b,i), 90° angles (Figure 6b,ii), and, permanent twists (Figure 6b,iii). This last demonstration goes beyond traditional origami folding, showing that this variable stiffness material is capable of twist-and-hold as well as bend-and-hold operations (see also Video S4, Supporting Information). We made several of these samples to test the ability of the material system to undergo several different shape changes, like tighter twists and being crumpled by hand (Figure 6c). Though these shape-changes could be reversed, the 3D printed PLA did not prove to be a very good variable-stiffness material in this regard as it remained permanently deformed from where it was forced to stretch. However, Taylor et al. recently demonstrated a simple chemical platform that enables the bonding of many types

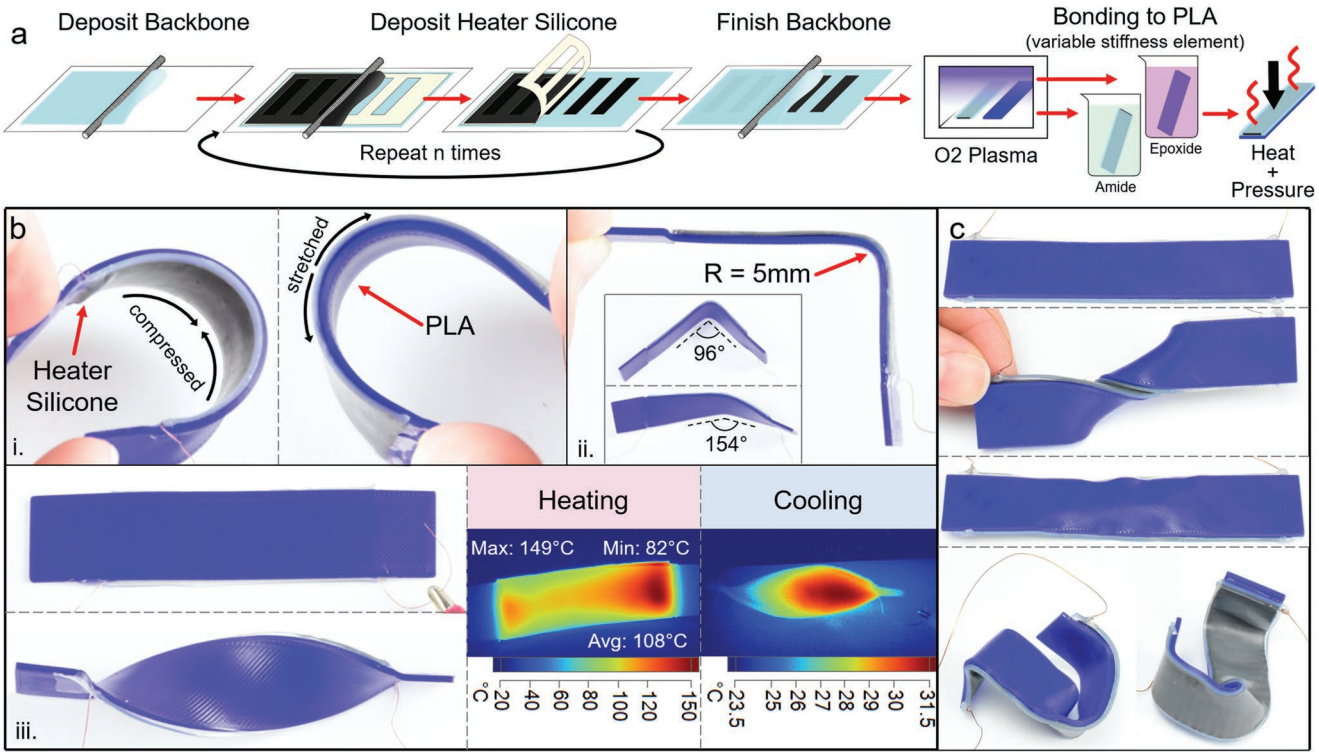

Figure 6. Reversible shape change. a) Manufacturing the heater silicone sheets with bonded variable stiffness elements (PLA). b) Heater silicone bonded to PLA is Joule heated enabling shape changing and holding operations in the PLA. b,i) The bond keeps the silicone connected to the PLA even when compressed and stretched. b,ii) A 90° fold in the variable stiffness sheet. Inset shows the shape-memory recovery of the material when Joule heated again. b,iii) The bonded system is given a permanent twist, with IR images of the sample as it is heated and cooled into the twisted shape. c) A second sample of the material undergoing a much tighter twist & hold (360°). After reheating, the PLA showed permanent warping. The heated system was then was crumpled to produce additional folds, twists, and bends, demonstrating the continued functionality of the heater silicone.

of commercial polymers (with glass transition temperatures <150 °C) to pure silicone, which could be employed to achieve material combinations that exhibit better performance.[50]

In Figure 6b,ii we also show that, due to both the elasticity of the silicone and the shape memory effect in the PLA variable stiffness sheet,[51,52] the material is able to recover some of the set shape when reheated after shape fixing. The ≈90° bend flattened itself, recovering 69% of its bend, and the twisted 180° sample was able to recover 66% of its twist (see also Video S4, Supporting Information). Though this effect is relatively weak, it is valuable to note that the bonded heater silicone can instigate this self-reversing shape change.

4.2. Reversible Hinges

To create reversible on-demand hinges in a stiff sheet, we combined the heater silicone, liquid metal wiring, and silicone-PLA bonding into a 1D, addressable, heating array with 5 liquid metal channels bonded to a variable stiffness sheet, creating 4 addressed variable stiffness "pixels" in a straight line (see **Figure 7**a,c). Each 1D pixel heating area in the heater silicone can be activated (i.e., the temperature raised to above 65 °C) independently or concurrently with other active pixels (see Figure 7b). This capability enables folds-on-demand in high-modulus thermoplastics. In Figure 7d, we show that by selectively engaging an individual pixel, we can bend the system on-demand at targeted locations while contacting the system at only a single point (i.e., a single fingertip). Since the rest of the system is rigid, only the targeted location bends under the input force (see inset to Figure 7d,ii–iii).

To demonstrate the versatility of a pixelized variable stiffness system, we formed several functional structures. We first formed the planar sheet into a load-bearing, raised cantilever (Figure 7d,ii). We then improved the load bearing design by adding another bend, turning the whole sheet into a raised table (see Figure 7d,ii and also Video S5, Supporting Information). Finally, we demonstrated that the reversibility of the pixels, as enabled by bonding the heater silicone to the variable stiffness sheet, allows the whole system to revert to its original shape. We did this by activating all the pixels simultaneously, and then manually flattening the system back into a straight plank (Figure 7e). It should be noted that the PLA sheet does not return to a pristine condition, as the heating and folding process naturally causes some warping in the re-flattened sheet, but regardless of this, the re-flattened plank could still support a mass (Figure 7f). This demonstration shows the possibilities for addressed fold-on-demand systems, as none of the load-bearing structures were preprogrammed into the material but formed by selectively heating one (or more) of four pixels. This concept can be further extended to joints-on-demand which has ramifications for controlling the active workspace of continuum manipulators.

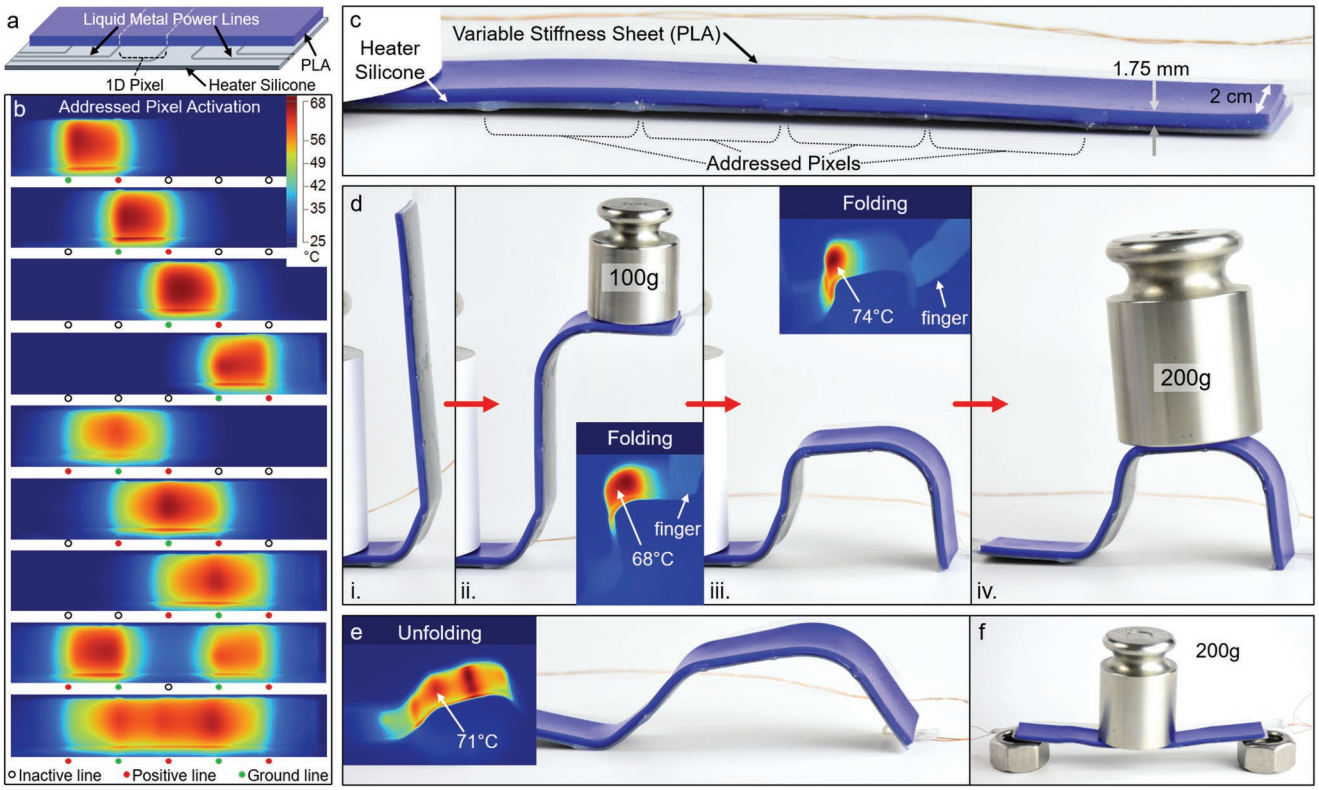

Figure 7. 1D pixelized addressable variable stiffness system. a) Schematic of the system demonstrating the various components allowing for addressable variable stiffness. b) IR images of the PLA side of the functional system with each pixel heated above the glass transition temperature (≈62 °C), showing the capability of a digitally controlled system to heat various pixels simultaneously. c) Visible light photo of the addressable system. d) The system undergoing shape changes into two load-bearing forms (see ii) and iv)) through heating of individual pixels. Insets in ii) and iii) show that the addressed pixel is the only heated point, allowing the system to be folded by a single finger. e) All pixels activated allowing the system to relax and be flattened into its original shape. f) The system, once cool, is again load bearing.

4.3. 2D On-Demand Hinges

Finally, returning to our initial motivation of "blank-slate" fold-on-demand, shape-changing structures, we used our 2D heating arrays to create some origami-like folding structures both adjacent to and bonded to the heating arrays (see **Figure 8**). In our first demonstration, we used the 4 × 5 addressable heater to fold a 2D sheet of PLA into a 3D "paper" airplane (see both Figure 8a,b and Video S6, Supporting Information). This was made possible by selectively heating both straight and diagonal lines using individual pixels in the heater, while the PLA sheet was placed on top of the silicone. We did not bond the array to the variable stiffness sheet, simply to allow for sharper folds.

To further illustrate the possibilities of a system that allows for folds-on-demand, with reversible folds, we bonded a sheet of PLA to the 6 × 6 addressable heater. This allowed us to use the 2D pixel array to create localized folding lines in the PLA sheet in multiple directions, as demonstrated in Figure 8c. As visible in the IR images in Figure 8c,ii, we observe that the pixels heated (≥62 °C) a spot with diameter 0.87 ± 0.11 cm. The spot size variation was due to the open-loop nature of the heating controller used. The center-to-center distance between diagonally adjacent pixels was 1.27 cm. Though the pixel density can be modulated, for our purposes the density of our 6 × 6 pixel array provided a good balance between the temperature required to heat each spot and the overlap between each pixel creating a continuous heated (softened) region. We demonstrate adding folds to the planar, stiff sheet, removing them to add additional folds, bi-directionality of the folds (a fold able to bend in both directions) and adding multiple folds at a time to a single sheet. For the sake of visibility, we held each fold partially open rather than having them completely flattened as in Figure 8b. These are just two demonstrations from the myriad possibilities of fold-on-demand sheet shaping via selective Joule heating.

5. Conclusion

We have developed a material-based tool to fill the need of a stretchable, addressable heater useful for controlling thermally responsive soft materials. We demonstrated a conductive heater silicone composite sheet that can heat an adjacent material to 150 °C and can be cyclically strained 1000 times at 40% strain while heating, due to reinforcement of the conductive silicone composite with an all-silicone backbone. This backbone became the key to successful implementation of localized, addressed heating within the heater silicone sheets, as well as both extend-and-hold demonstrations and fold-on-demand (shape

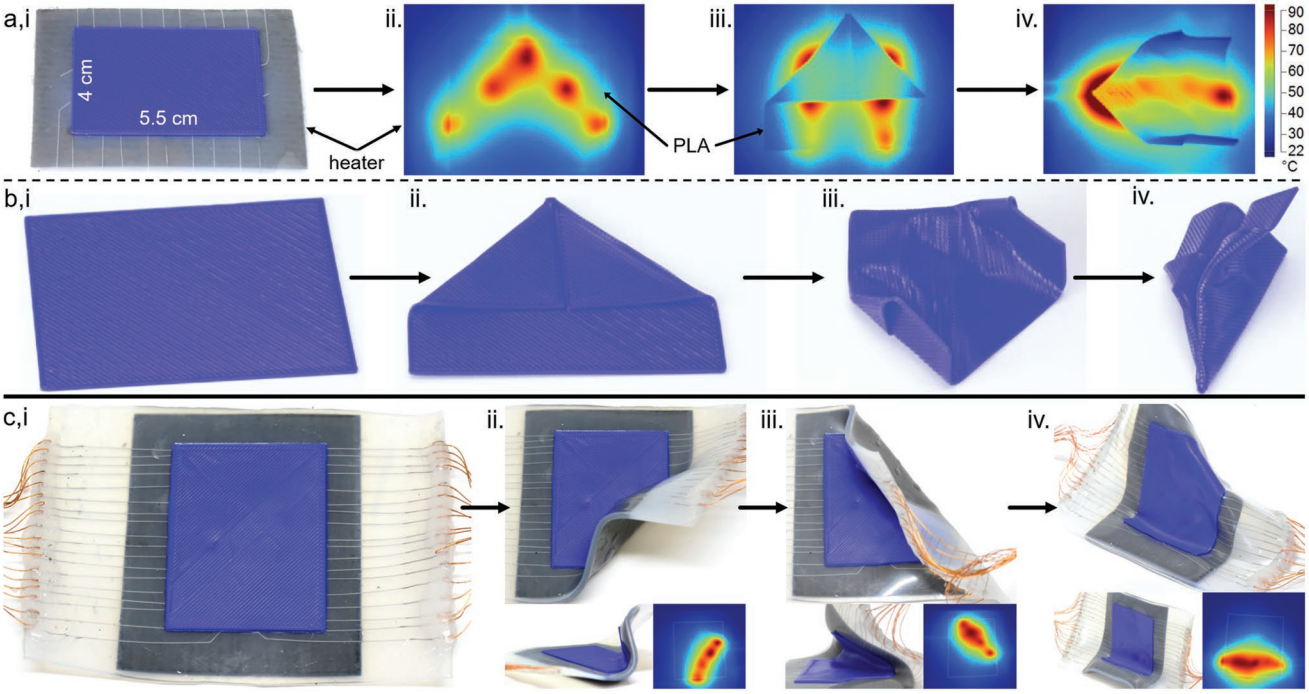

Figure 8. a-b) An unprogrammed variable stiffness sheet is heated using the 4 × 5 pixel heater to create artificial folds. a,i) The sheet laying on the heater. a,ii–iv) Top-down IR images showing the heated folds on the sheet. b) Images of the sheet in i) its initial state, ii-iii) intermediate states, and iv) final airplane-like shape after being cooled. c,i) PLA sheet bonded to a 6 × 6 pixel heater silicone sheet. c,ii–iv) The PLA sheet is bent (and flattened) along lines not previously defined in the polymer block, simply by heating a selection of pixels that make up a line with the heater silicone sheet. In both ii) and iii) the top view and a side-profile view of two successive bends are presented, along with an IR photo just before the bend occurred with the PLA sheet outlined. iv) An isometric view showing multiple bends in the same sheet, as well as an isometric view of the initial straight-line bend on the bottom (with its associated IR image). All IR images show temperatures up to 90 °C. All PLA sheets are 4 cm × 5.5 cm.

changing) structures. The backbone was critical to successful implementation of addressed heating pixels as it carries stretchable liquid metal electrode channels out-of-plane, until the electrode is ready for interfacing at specific locations in the heater silicone. We demonstrated a 6 × 6 array of heating pixels with a density of 1.9 pixels cm^{-2}, with each pixel able to (via open-loop control) heat up and soften an ≈0.87 cm diameter spot in adjacent PLA sheets. By introducing closed-loop control on the power being passed through each addressable pixel (rather than the current open-loop state) we envision future work in which the local temperature can be far more precisely controlled, enabling uniform, gradient, or targeted heating. Although the backbone underpins the stretchability of the heater silicone, manufacturing of the composite layer also had a large impact on the uniformity of the heating and the stretchability of the sample. In future work, we aim to improve the thermal conductivity of the system so that the heater silicone is able to self-regulate the heat and distribute it more evenly around each point and swath.

The silicone backbone also allows for strong bonding to both a wax silicone composite and variable-stiffness polymer sheets to create composite material sheets which can change their stiffness on-demand. With the wax silicone, we were able to illustrate the potential of an all-silicone, bulk material, planar heater by performing stretch-and-hold operations, which can potentially open a whole new frontier of planar material reconfiguration in which parts of the plane can be made stretchable. Future work in this area will involve balancing the force the wax-silicone exerts when in its extended-and-held state with the heater silicone's restoring force, so that the system can remain both elongated and flat. We envision the methods presented here used to create ready-to-use slates that can be stretched, folded, twisted, and formed into complex 3D structures using pixel-controlled soft "origami" folding in an otherwise blank material.

6. Experimental Section

Materials: Dragonskin 10 (Smooth-On Inc.) was used as the silicone for all experiments. Variable stiffness sheets were FDM 3D printed polylactic acid (PLA) sheets. This allowed for control over all three dimensions (length, width, and height) in the variable stiffness sheets for the various applications and demonstrations. Paraffin wax (melting temperature 60–65 °C) was used as the stiffness changing filler in the stretch-and-hold silicone examples. It was mixed into the silicone matrix in a 1:2 ratio (33.3% wax by weight).

Expanded intercalated graphite composite was prepared by first exfoliating graphene sheets from graphite flakes and second, mixing it into the composite via a solvent carrier. 10 g of dry expandable graphite (Sigma-Aldrich) was heated in an oven at 800 °C, causing the exfoliation of the graphene flakes into noodle-like, ultra-low-density structures in ≈20 s. These noodles were soaked in cyclohexane (BDH1111, VWR) and sonicated for 4 h (Q700 sonicator fitted with 1/2" tip, QSonica, 20 kHz, 36 µm (30% setting) amplitude) creating

a slurry of solvent and individual EIG particles. The slurry was allowed to settle, and excess solvent was decanted off until the solution had a ratio between 3 and 5 wt% EIG, giving it a paste-like consistency. To finish the composite, equal parts A and B of the silicone elastomer were premixed and chilled to prevent premature crosslinking. A few grams of this mixture were added to the EIG, according to the final desired mix ratio and volume of composite, and the whole solution was mixed thoroughly. The composite was then rod-coated into sheets, allowing the remaining cyclohexane solvent to evaporate away. Subsequent layers were rod-coated after the previous layer had fully cured.

Thermally responsive color-changing silicone (for Figure 3c) was made by adding a thermochromatic additive powder (Hali Industrial Co., Ltd.) to the silicone. The material began to exhibit a visible color change at ≈30 °C, though higher temperatures caused a more distinct change.

Strain Testing: A heater silicone specimen was cyclically strained in an Instron 3345 materials tester while measuring the resistance across the sample. The active (stretched) area of samples tested was 10 cm long, 1 cm wide, with a conductive layer <300 µm thick. The strain test procedure was as follows: samples were cyclically strained to 10% strain 200 times at 200 mm min^{-1}. The samples were then strained at incrementally higher strain values for 50 cycles per increment (5% strain increase per increment, making the test 15%, 20%, 25%, etc.) for 50 cycles at each strain value up to 50% strain.

Cyclic Heat Testing: Heater silicone was cyclically strained in a custom test apparatus, while maintaining an elevated, Joule heated temperature. The electrically active area (between two liquid metal electrodes) was 3 cm × 1 cm, and was strained at a strain rate of 35 mm min^{-1}.

Supporting Information

Supporting Information is available from the Wiley Online Library or from the author.

Acknowledgements

The authors would like to thank Dr. Edward L. White for his contributions to preliminary studies leading up to this work, including his help designing the circuit boards used to power the addressed silicone heaters. R.A.B. was funded by an AFOSR Young Investigator award (Grant No. FA9550-16-1-0267) and by a NASA Early Career Faculty award (Grant No. NNX14AO52G). M.C.Y. was supported under the National Science Foundation Graduate Research Fellowship program (DGE-1333468). Any opinions, findings, and conclusions or recommendations expressed in this material are those of the authors and do not necessarily reflect the views of the US Air Force Office of Scientific Research, the National Aeronautics and Space Administration, or the National Science Foundation.

Conflict of Interest

The authors declare no conflict of interest.

Keywords

local thermal control, stretchable conductive composites, stretchable heaters, variable stiffness systems

Received: April 1, 2019
Revised: June 5, 2019
Published online: August 2, 2019

[1] M. Calisti, G. Picardi, C. Laschi, *J. R. Soc., Interface* **2017**, *14*, 20170101.
[2] F. Ilievski, A. D. Mazzeo, R. F. Shepherd, X. Chen, G. M. Whitesides, *Angew. Chem., Int. Ed.* **2011**, *50*, 1890.
[3] E. W. Hawkes, L. H. Blumenschein, J. D. Greer, A. M. Okamura, *Sci. Rob.* **2017**, *2*, eaan3028.
[4] D. Drotman, S. Jadhav, M. Karimi, P. deZonia, M. T. Tolley, in *2017 IEEE International Conference on Robotics and Automation (ICRA)*, **2017**, pp. 5532–5538.
[5] J. Hughes, U. Culha, F. Giardina, F. Guenther, A. Rosendo, F. Iida, *Front. Rob. AI* **2016**, *3*, 69.
[6] M. Manti, V. Cacucciolo, M. Cianchetti, *IEEE Rob.Autom. Mag.* **2016**, *23*, 93.
[7] T. P. Chenal, J. C. Case, J. Paik, R. K. Kramer, in *2014 IEEE/RSJ International Conference on Intelligent Robots and Systems*, **2014**, pp. 2827–2831.
[8] L. Wang, Y. Yang, Y. Chen, C. Majidi, F. Iida, E. Askounis, Q. Pei, *Mater. Today* **2018**, *21*, 563.
[9] S. M. Felton, M. T. Tolley, B. Shin, C. D. Onal, E. D. Demaine, D. Rus, R. J. Wood, *Soft Matter* **2013**, *9*, 7688.
[10] A. Miriyev, K. Stack, H. Lipson, *Nat. Commun.* **2017**, *8*, 596.
[11] L. Blanc, A. Delchambre, P. Lambert, *Actuators* **2017**, *6*, 23.
[12] T. L. Buckner, E. L. White, M. C. Yuen, R. A. Bilodeau, R. K. Kramer, in *2017 IEEE/RSJ International Conference on Intelligent Robots and Systems (IROS)*, **2017**, pp. 3728–3733.
[13] M. Yuen, R. A. Bilodeau, R. Kramer, *IEEE Rob. Autom. Lett.* **2016**, *1*, 708.
[14] M. Taghavi, T. Helps, B. Huang, J. Rossiter, *IEEE Rob. Autom. Lett.* **2018**, *3*, 2402.
[15] S. Rich, S.-H. Jang, Y.-L. Park, C. Majidi, *Adv. Mater. Technol.* **2017**, *2*, 1700179.
[16] R. A. Bilodeau, A. Miriyev, H. Lipson, R. Kramer-Bottiglio, in *2018 IEEE International Conference on Soft Robotics (RoboSoft)*, **2018**, pp. 288–294.
[17] E.-S. Park, L. Wook Jang, J.-S. Yoon, *J. Appl. Polym. Sci.* **2005**, *95*, 1122.
[18] J. Kang, H. Kim, K. S. Kim, S.-K. Lee, S. Bae, J.-H. Ahn, Y.-J. Kim, J.-B. Choi, B. H. Hong, *Nano Lett.* **2011**, *11*, 5154.
[19] D. Sui, Y. Huang, L. Huang, J. Liang, Y. Ma, Y. Chen, *Small* **2011**, *7*, 3186.
[20] B. W. An, E.-J. Gwak, K. Kim, Y.-C. Kim, J. Jang, J.-Y. Kim, J.-U. Park, *Nano Lett.* **2016**, *16*, 471.
[21] J. Jang, B. G. Hyun, S. Ji, E. Cho, B. W. An, W. H. Cheong, J.-U. Park, *NPG Asia Mater.* **2017**, *9*, e432.
[22] N. Lazarus, B. Hanrahan, *Adv. Mater. Technol.* **2016**, *1*, 1600130.
[23] Y. Li, Z. Zhang, X. Li, J. Zhang, H. Lou, X. Shi, X. Cheng, H. Peng, *J. Mater. Chem. C* **2017**, *5*, 41.
[24] R. C. Webb, A. P. Bonifas, A. Behnaz, Y. Zhang, K. J. Yu, H. Cheng, M. Shi, Z. Bian, Z. Liu, Y.-S. Kim, W.-H. Yeo, J. S. Park, J. Song, Y. Li, Y. Huang, A. M. Gorbach, J. A. Rogers, *Nat. Mater.* **2013**, *12*, 938.
[25] J. A. Fan, W.-H. Yeo, Y. Su, Y. Hattori, W. Lee, S.-Y. Jung, Y. Zhang, Z. Liu, H. Cheng, L. Falgout, M. Bajema, T. Coleman, D. Gregoire, R. J. Larsen, Y. Huang, J. A. Rogers, *Nat. Commun.* **2014**, *5*, 3266.
[26] L. Zhang, M. Baima, T. L. Andrew, *ACS Appl. Mater. Interfaces* **2017**, *9*, 32299.
[27] S. Choi, J. Park, W. Hyun, J. Kim, J. Kim, Y. B. Lee, C. Song, H. J. Hwang, J. H. Kim, T. Hyeon, D.-H. Kim, *ACS Nano* **2015**, *9*, 6626.
[28] S. Hong, H. Lee, J. Lee, J. Kwon, S. Han, Y. D. Suh, H. Cho, J. Shin, J. Yeo, S. H. Ko, *Adv. Mater.* **2015**, *27*, 4744.
[29] Y. Wang, Z. Yu, G. Mao, Y. Liu, G. Liu, J. Shang, S. Qu, Q. Chen, R.-W. Li, *Adv. Mater. Technol.* **2018**, *0*, 1800435.
[30] D. Kim, L. Zhu, D.-J. Jeong, K. Chun, Y.-Y. Bang, S.-R. Kim, J.-H. Kim, S.-K. Oh, *Carbon* **2013**, *63*, 530.

[31] A. C. Siegel, S. T. Phillips, B. J. Wiley, G. M. Whitesides, *Lab Chip* **2009**, *9*, 2775.
[32] P. Liu, L. Liu, K. Jiang, S. Fan, *Small* **2011**, *7*, 732.
[33] H. Kim, H. Lee, I. Ha, J. Jung, P. Won, H. Cho, J. Yeo, S. Hong, S. Han, J. Kwon, K.-J. Cho, S. H. Ko, *Adv. Funct. Mater.* **2018**, *28*, 1801847.
[34] E. A. Allen, J. P. Swensen, *Actuators* **2018**, *7*, 80.
[35] D. McCoul, S. Rosset, N. Besse, H. Shea, *Smart Mater. Struct.* **2017**, *26*, 025015.
[36] S. Puce, T. Dattoma, F. Rizzi, M. Emara, A. Qualtieri, M. De Vittorio, *Microelectron. Eng.* **2019**, *205*, 6.
[37] M. A. McEvoy, N. Correll, *J. Compos. Mater.* **2015**, *49*, 1799.
[38] N. Besse, S. Rosset, J. J. Zarate, H. Shea, *Adv. Mater. Technol.* **2017**, *2*, 1700102.
[39] M. Cai, D. Thorpe, D. H. Adamson, H. C. Schniepp, *J. Mater. Chem.* **2012**, *22*, 24992.
[40] D. D. L. Chung, *J. Mater. Sci.* **2016**, *51*, 554.
[41] W. Zhang, A. A. Dehghani-Sanij, R. S. Blackburn, *J. Mater. Sci.* **2007**, *42*, 3408.
[42] R. Verdejo, M. M. Bernal, L. J. Romasanta, M. A. Lopez-Manchado, *J. Mater. Chem.* **2011**, *21*, 3301.
[43] M. Kujawski, J. D. Pearse, E. Smela, *Carbon* **2010**, *48*, 2409.
[44] K. K. Sadasivuni, D. Ponnamma, S. Thomas, Y. Grohens, *Prog. Polym. Sci.* **2014**, *39*, 749.
[45] E. L. White, M. C. Yuen, J. C. Case, R. K. Kramer, *Adv. Mater. Technol.* **2017**, *2*, 1700072.
[46] M. D. Dickey, *Adv. Mater.* **2017**, *29*, 1606425.
[47] M. D. Dickey, *ACS Appl. Mater. Interfaces* **2014**, *6*, 18369.
[48] B. Li, Y. Gao, A. Fontecchio, Y. Visell, *Smart Mater. Struct.* **2016**, *25*, 075009.
[49] S. A. Morin, R. F. Shepherd, S. W. Kwok, A. A. Stokes, A. Nemiroski, G. M. Whitesides, *Science* **2012**, *337*, 828.
[50] J. M. Taylor, K. Perez-Toralla, R. Aispuro, S. A. Morin, *Adv. Mater.* **2018**, *30*, 1705333.
[51] F. S. Senatov, K. V. Niaza, M. Y. Zadorozhnyy, A. V. Maksimkin, S. D. Kaloshkin, Y. Z. Estrin, *J. Mech. Behav. Biomed. Mater.* **2016**, *57*, 139.
[52] S. K. Leist, D. Gao, R. Chiou, J. Zhou, *Virtual Phys. Prototyping* **2017**, *12*, 290.